SEMARAK ILMU PUBLISHING

Journal of Advanced Research in Fluid Mechanics and Thermal Sciences

Journal homepage:
https://semarakilmu.com.my/journals/index.php/fluid_mechanics_thermal_sciences/index
ISSN: 2289-7879

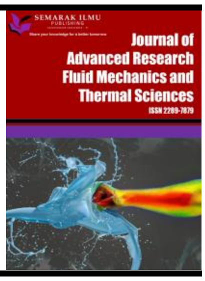


# Assessment of Photovoltaic Thermal Efficiency using Phase Change Material and Water-Channel Collector with T-Fin Design

Low Zi Qing[1], Mohd Afzanizam Mohd Rosli[1,*], Nurfarhana Salimen[1], Azrin Hani Abdul Rashid[2], Safarudin Gazali Herawan[3]

[1] Faculty of Mechanical Technology and Engineering, Universiti Teknikal Malaysia Melaka, Hang Tuah Jaya, 76100 Durian Tunggal, Melaka, Malaysia
[2] Faculty of Engineering Technology. Universiti Tun Hussein Onn Malaysia (UTHM), 84600 Pagoh, Muar, Johor, Malaysia
[3] Industrial Engineering Department, Faculty of Engineering, Bina Nusantara University, Jakarta, 11430, Indonesia

**ARTICLE INFO**

***Article history:***
Received 9 August 2024
Received in revised form 11 November 2024
Accepted 23 November 2024
Available online 10 December 2024

***Keywords:***
Photovoltaic thermal; phase change material; T-fin absorber

**ABSTRACT**

Photovoltaic thermal systems, also known as hybrid solar panels, combine photovoltaic and solar thermal components to generate both electrical and heat energy from the sun. Despite solar energy has significant potential, conventional photovoltaic systems suffer from low efficiencies due to the wasted heat energy and high working temperature. This research aims to develop and examine the efficiency of a photovoltaic thermal system integrated with commercial phase change material (PCM) using copper T-fin absorber to increase solar energy conversion efficiency. The research involved fabricating aluminium packets for commercial PCM, filling fabricated packets into a developed photovoltaic thermal system with T-fin absorber, and conducting final experiments under three different water flow rates for each of three different irradiance levels under solar simulator with 30 minutes run for each test. The final experiment assessed temperature difference, electrical efficiency, thermal efficiency, and overall efficiency. At 800 W/m² and 90 l/h, the highest temperature drop was 11.20°C. The highest electrical efficiency of 8.0% was achieved at 800 W/m² and 90 l/h. The highest thermal efficiency was 72.5% at 400 W/m² and 90 l/h. The highest overall efficiency of 79.8% at 400 W/m² and 90 l/h for the T-fin absorber. These results concluded the enhanced heat transfer capability and contribution to higher overall system efficiency after integrated commercial PCM and T-fin absorber.

## 1. Introduction

The growing global demand for clean and sustainable energy has accelerated research and development in the field of solar energy. In recent years, efforts have been made to increase the efficiency of solar energy conversion into electricity using conventional photovoltaic modules. Nevertheless, the electrical efficiency or energy conversion efficiency ($\eta_{El}$) of photovoltaic modules is

* *Corresponding author.*
*E-mail address: afzanizam@utem.edu.my*

https://doi.org/10.37934/arfmts.125.1.7593

currently only achieved by 15-20%, largely due to heat energy losses and elevated operating temperatures that degrade the performance of photovoltaic modules [1].

Photovoltaic thermal (PVT) systems, also known as hybrid solar panels, represent an innovative and advanced solution to enhance the efficiency of solar energy systems [2]. By combining photovoltaic (PV) and solar thermal components (T), PVT systems generate both electrical and thermal energy from the sun [3]. This dual-generation capability allows PVT systems to utilize excess heat energy that is usually wasted in conventional PV systems, thereby improving overall power output and efficiency [4]. Liquid-type PVT systems can achieve thermal efficiency between 22.9% and 33.3% [5].

The integration of phase change material (PCM) is one of the innovative passive cooling methods to further enhance the efficiency of PVT systems [6]. The PCM can store and release large amounts of thermal energy during phase transitions, such as from solid to liquid and vice versa [7]. This unique property allows PCM to manage thermal energy effectively, storing excess heat during daytime periods and releasing heat needed at night [8]. This cooling method can enhance thermal regulation, reduce overheating of photovoltaic systems, and improve overall system performance [9]. The integration of PCM increased electrical efficiency by 5.9% and reduced module temperature by 24% [10].

Metal fins made from materials with high thermal conductivity such as aluminium or copper are used to enhance heat dissipation in PVT systems [11]. These fins are attached to the rear side of the PV modules, increasing the surface contact area available for heat transfer [12]. The increased surface contact area allows for more efficient dissipation of the heat generated by the PV cells, which can reduce the operating temperature and improve the electrical efficiency of the system [13]. There are multiple designs and arrangements of metal fins, but one of the effective configurations is the T-fin absorber, with enhanced heat transfer properties, and able to lower PV temperatures by 9.82%, significantly boosting system performance [14].

To further enhance the efficiency of photovoltaic thermal systems, research was conducted on the integration of PCM with a T-fin absorber and varying the mass flow rate of water with constant solar irradiance. Several researchers who have conducted similar research by using PVT systems integrated with PCM and fin absorber are summarized in Table 1.

Based on the literature review, the integration of PCM and fins in PVT systems has proven to be an effective passive cooling method for enhancing both thermal and electrical efficiencies. These studies show significant improvements in temperature management and solar energy conversion can be achieved by optimizing the configuration and materials used. The combination of PCM and fins enhances the passive cooling capacity of PVT systems. PCM absorbs excess heat and reduces the working temperature of the PV modules, while fins increase the surface area for heat dissipation. Different PCMs (e.g., white petroleum jelly, paraffin wax, RT35, nano PCM) have different melting temperatures and thermal properties which can influence the efficiency gains. The option of fin design (e.g., triangular-shaped, external, micro-fin tube) also plays a critical role in heat transfer efficiency. The performance of PVT systems varies significantly based on testing conditions (indoor or outdoor) and geographical location which can lead to a huge range of solar irradiance and ambient temperature. Higher mass flow rates contribute to better heat removal, this can be seen in the studies by Hamada *et al.,* [19] which recorded higher efficiency gains with increased water flow rates. The largest difference in overall efficiency enhanced between 3% and 62.1% is due to the PV module with or without a solar thermal collector. This water-channel-based solar thermal allows to capture of the wasted heat energy and convert it to become useful energy, therefore the overall efficiency can be significantly increased due to a combination of electrical and thermal efficiencies instead of electrical efficiency only.

**Table 1**
Previous work on PVT integrated with PCM

| Cell Panel | PCM | Absorber | Melting Point of PCM | Solar Irradiance | Mass Flow Rate | Location | Temp. Drop | Overall Efficiency Enhanced | Ref. |
|---|---|---|---|---|---|---|---|---|---|
| PVT (Water) | White Petroleum Jelly | Triangular Shaped Fin | 36-60°C | - | 0.0013 kg/s | Outdoor, India | 8.10% | 49.99% | [15] |
| PVT (nanofluid ZnO+Water) | RT35 | Copper Foam System | 29-36°C | 1000 W/m$^2$ | 0.0083-0.017 kg/s | Numerical Simulation | 11% | 29.3% | [16] |
| PVT (nanofluid with 0.6 vol% SiC) | Nano PCM (SiC 1% Vol) | Micro-Fin Tube | - | 800 W/m$^2$ | 0.041 kg/s | Indoor, Malaysia | 25.12% | 53.9% | [17] |
| PVT (Hybrid Air-Water) | Paraffin Wax | Tube water+Air collector | 46-48°C | 300-1200 W/m$^2$ | 0.01 -0.05 kg/s | Outdoor, Iraq | 43.33% | 93.64% | [18] |
| PVT (Water) | RT35 | Fin | 32-38°C | 682-782 W/m$^2$ | 0.05 kg/s | Outdoor, Egypt | 16.9% | 62.1% | [19] |

This study distinguishes itself from comparable research by focusing on a copper T-fin absorber with commercial PCM integration, as opposed to using advanced cooling fluids like nanofluids or more complex fin geometries such as micro-fin tubes or triangular fins. While nanofluids may enhance heat transfer due to their improved thermal properties, nanofluids often require precise fluid dynamics control and can be costlier and more complex to implement. Similarly, micro-fin or triangular fin designs could offer enhanced heat transfer by increasing the surface area and turbulence but tend to involve more intricate manufacturing processes and may not provide as balanced a solution between electrical and thermal efficiency as the T-fin design used in this study. The T-fin absorber design offers a simpler, cost-effective solution while still achieving substantial heat dissipation and performance improvements without the added complexity of alternative cooling techniques.

Despite the advancements in PVT systems, a significant gap remains in optimizing the integration of PCMs and fin designs to maximize efficiency under varying operational conditions such as applying multiple water flow rates at constant solar irradiance levels. Most studies focus on specific configurations or single environmental factors, missing a need for comprehensive research that evaluates multiple variables simultaneously. The lack of T-shaped fins as passive cooling applications in PVT systems is also an inspiration for conducting this research. This research is significant as it aims to bridge this gap by developing a PVT system integrated with commercial PCM and a copper T-fin absorber, analyzing the performance under constant solar irradiance and varying water mass flow rates. The findings of this research will contribute to the broader body of knowledge by providing suggestions for the most effective configurations and operational parameters for maximizing the efficiency of PVT systems. The objective of this research is to develop and evaluate the efficiency of a photovoltaic thermal system integrated with commercial PCM using a copper T-fin absorber by aiming to enhance solar energy conversion efficiency. This will involve fabricating and integrating the components, followed by performance testing under controlled conditions to assess temperature difference, electrical efficiency, thermal efficiency, and overall system efficiency.

## 2. Methodology

### *2.1 Fabrication of PCM Packet*

The commercial phase change material (PCM) selected for this study exhibits a melting point and latent heat capacity that are well-suited for solar energy applications causing effective thermal energy storage. The thermal stability across various temperature ranges maintains consistent performance. Alternative PCMs, such as paraffin or organic materials may present different melting points and thermal characteristics, which could affect the overall efficiency of the system. For instance, paraffin may offer higher latent heat but could also have lower thermal conductivity compared to the chosen PCM, potentially causing in less effective heat transfer and slower melting rates. Thus, the selected PCM optimizes the performance of the integrated PVT system by balancing these crucial thermal properties.

To enhance the efficiency of PVT systems, PCM packets were fabricated using black aluminum to optimize thermal management through latent heat storage. Black aluminum was chosen for the fabrication of the PCM packets due to favorable thermal properties, such as high thermal conductivity, corrosion resistance, and durability. Additionally, the black surface enhances solar absorption, further improving heat transfer to the PCM. Other materials and designs were considered, such as copper or composites, which offer higher thermal conductivity. However, copper was not selected due to its higher cost and weight, which could impact the overall efficiency and economic viability of the system. To further improve system longevity, alternative designs like finned or ribbed packets may also enhance heat transfer by increasing the surface area, although these designs would require more complex fabrication techniques. Future studies could explore these materials and designs to optimize both heat transfer and durability. According to Table 2, the PCM quantity required was calculated and volume expansion when heated was accounted. Black aluminum was chosen due to the high thermal conductivity. The packets were customized to fit the T-Fin absorber design and dimensions in Table 3 and Figure 1, which are 5x20 cm for the bottom layer and 13x20 cm for the upper layer. Before filling, the PCM was grated into smaller pieces as shown in Figure 2. Each packet was filled with the required PCM mass, sealed, and vacuumed to ensure no leaks during operation. A rigorous leak test validated the durability of packets under high temperatures. In total, 24 packets were fabricated for the bottom layer and 9 for the upper layer to ensure efficient heat transfer and optimal performance of the PVT system. Based on Table 4, a total of 1.5kg PCM filled in 33 PCM packets were used, and the fabricated aluminum packets are shown in Figure 3.

**Table 2**
Mass of PCM required in liquid and solid state

| Item | Value | Unit |
|---|---|---|
| Melting temperature | 40-43.5 | °C |
| Latent heat of fusion of PCM, $H_m$ | 175.77 | kJ/kg |
| Density of PCM, ρ | 845 | kg/m$^3$ |
| Volume available in PVT container, V | 0.001976 | m$^3$ |
| Mass of PCM required (liquid-state), $m_{pcm,liquid}$ | 1.67 | kg |
| Volume expansion | 10 | % |
| Mass of PCM required (solid-state), $m_{pcm,solid}$ | 1.50 | kg |

**Table 3**
Dimension of T-fin absorber

| Item | Quantity | Value | Unit |
|---|---|---|---|
| Height of T-fin | 13 | 0.02 | m |
| Length of long T-fin | 11 | 0.35 | m |
| Length of short T-fin | 2 | 0.24 | m |
| Width of T-fin between tip to tip | 12 | 0.027 | m |
| Width of T-fin between inner gap | 12 | 0.045 | m |

**Table 4**
Dimension and size of PCM packets

| Size | Material | Length | Width | Location | Mass of PCM | Quantity | Total mass |
|---|---|---|---|---|---|---|---|
| Small | Aluminium | 20cm | 5cm | Bottom | 20g | 24 | 480g |
| Large | Aluminium | 20cm | 13cm | Upper | 113.33g | 9 | 1020g |
| Total | | | | | | 33 | 1500g |

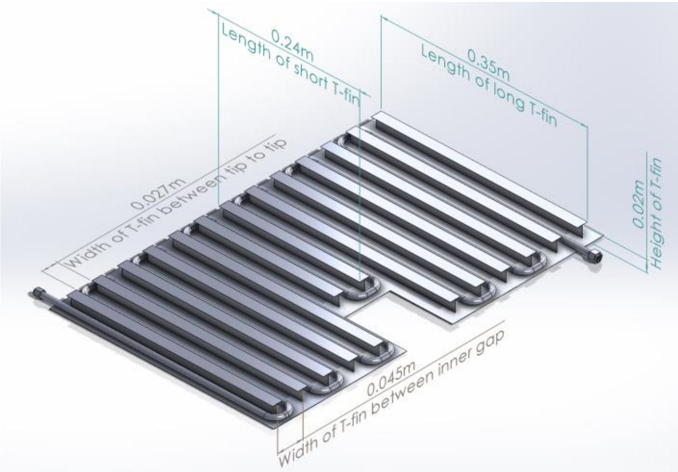


**Fig. 1.** Dimensions of T-fin absorber

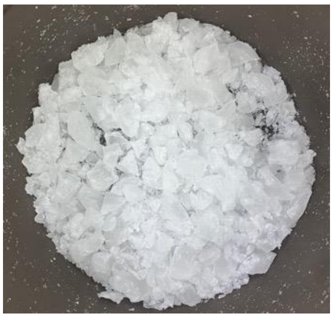

**Fig. 2.** PCM grated into small pieces

**Fig. 3.** Fabricated PCM packets

### *2.2 Fabrication of PVT System*

The PVT system was designed with a T-fin absorber and integrated with commercial PCM to enhance thermal management. In designing the T-fin absorber, copper was chosen for high thermal conductivity which approximately 400 W/mK, which enhances heat absorption from solar radiation and promotes efficient heat transfer to the PCM. Although aluminum about 235 W/mK was considered for the cost and weight benefits, aluminum was less effective for this application. Given excellent thermal properties of copper, no additional materials were incorporated to improve conductivity, as copper sufficiently meets the thermal requirements for optimal PCM melting and overall system efficiency. The insulation cover of the PV module was removed to install the T-fin absorber, and aluminum PCM packets in Figure 4 were inserted to improve heat transfer during melting. The insulation cover was resealed with silicone sealant to prevent leaks. Water-channel inlets and outlets were secured with anti-leak tape to maintain a constant water flow rate as shown in Figure 5. The fully assembled PVT system with integrated PCM and T-fin absorber ensures efficient heat management and was prepared for various water flow rate tests at a constant irradiance level as shown in Figure 6. The specification of the PV module from the manufacturer is listed in Table 5.

(a) (b)

**Fig. 4.** Aluminum PCM packets were inserted into the container (a) Bottom layer, (b) Upper layer

**Fig. 5.** Anti-leaking white tape tied on water inlet and outlet

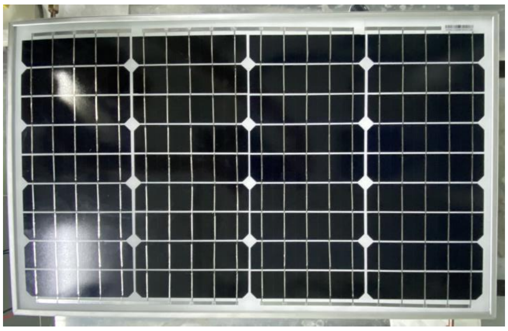

**Fig. 6.** Fully assembled PVT system

**Table 5**
PV Module at Standard Testing condition (STC)

| Specification | Value |
|---|---|
| Model type | SW40M-36 |
| Maximum Output Power ($P_{mp}$) | 40W |
| Maximum Power Voltage ($V_{mp}$) | 18.0V |
| Maximum Power Current ($I_{mp}$) | 1.11A |
| Open Circuit Voltage ($V_{oc}$) | 21.6V |
| Short Circuit Current ($I_{sc}$) | 1.19A |
| Size (Dimension) | 670*420*25mm |
| Weight | 1.7kg |
| Output Tolerance | 0 - +5W |
| Standard Test Condition (STC) | 1000W/m$^2$, AM 1.5, 25°C |
| Operating Temperature | -40°C ~ +85°C |

In this study, both vertical and horizontal oscillations were implemented to enhance the melting efficiency of the phase change material (PCM) integrated within the PVT system. The vertical oscillation was chosen to promote natural convection currents, facilitating improved heat distribution and more uniform melting of the PCM. This motion enables the PCM to effectively absorb heat from the copper T-fin absorber. Conversely, horizontal oscillation was employed to encourage lateral fluid movement, which mitigates thermal stratification and enhances heat transfer rates by ensuring that cooler PCM is brought into contact with warmer regions. Other potential oscillation directions, such as diagonal oscillations, were considered during the design phase but were ultimately excluded due to the complexities they introduced in flow dynamics and the risk of creating turbulence that could adversely affect PCM melting. The combination of vertical and horizontal oscillations thus provided a balanced approach to maximizing the thermal performance of the PVT system.

### *2.3 Final Experiment Setup*

A controlled environment was created to test the PVT system under constant irradiance and varying water mass flow rates. The setup included placing the PVT module on a workbench, connecting a 5L distilled water tank to a Verderflex pump, a flow meter, and the PVT water channel, with a heat exchanger cooling the discharged hot water. Type-K thermocouples measured temperature differences at the PVT inlet and outlet, while six surface temperature sensors recorded data via a TC-08 Thermocouple Data Logger. A pyranometer measured solar irradiance, and PV cables connected to an Array 3721A DC Electronic Load analyzed electrical parameters. Figure 7 shows schematic view of the experiment setup. The experiment tested different cell panel systems (PV module alone, PVT with PCM and T-Fin absorber) at various irradiance levels (400W/m², 600W/m², and 800W/m²) and water flow rates (30 l/h, 60 l/h, and 90 l/h) for 30 minutes each. The irradiance levels of 400 W/m², 600 W/m², and 800 W/m² reflect typical real-world solar conditions, from cloudy to clear skies. Higher irradiance increases energy absorption which can improving thermal and electrical performance. However, excessive irradiance can raise temperatures which can lower electrical efficiency. Hence, the effective cooling that integrated in this system is also important. A setup process flow is shown in Figure 8.

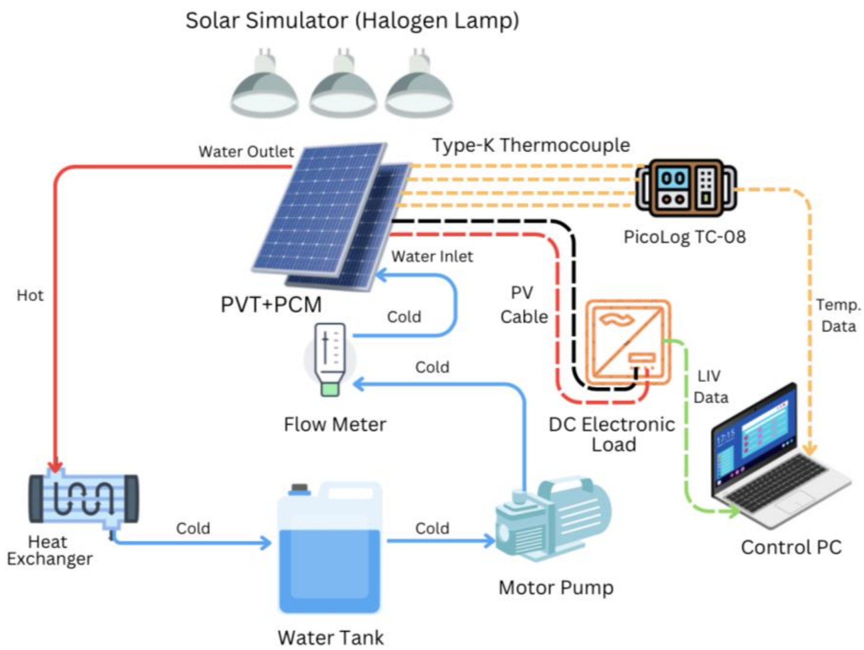


**Fig. 7.** Schematic diagram of experiment setup

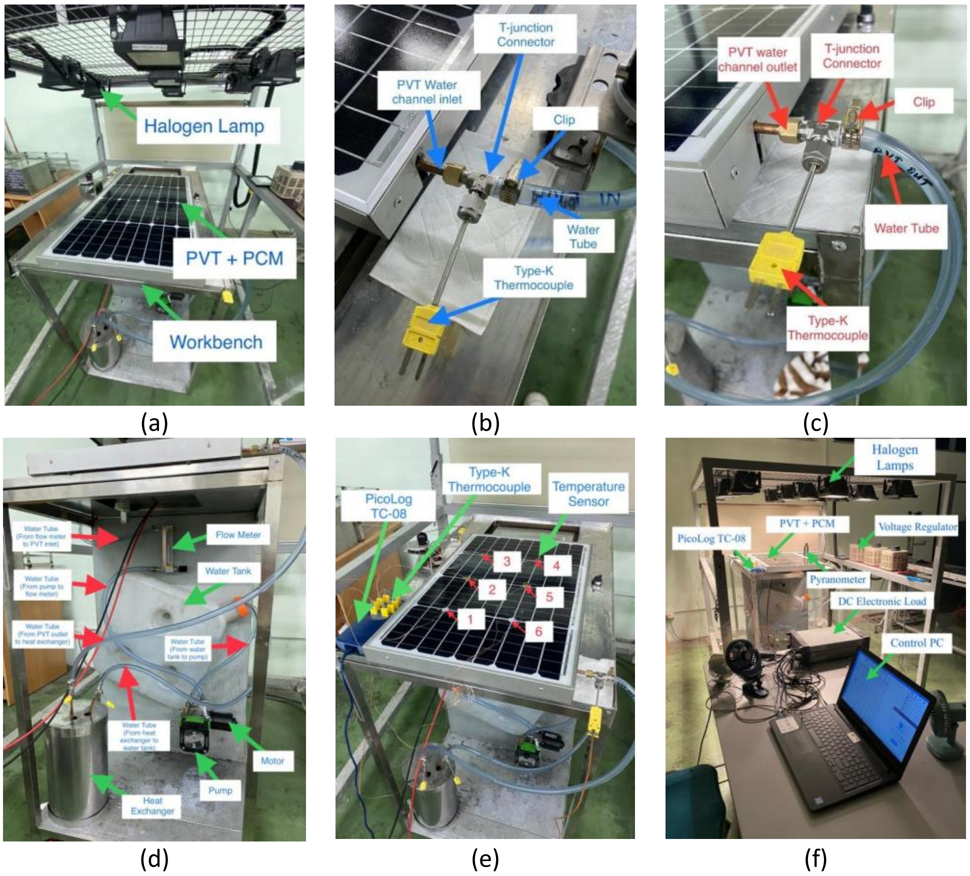


**Fig. 8.** Process flow of final experiment setup (a) PVT module, (b) Water channel inlet, (c) Water channel outlet, (d) Water flow setup, (e) Thermocouple setup, (f) Final setup

### *2.4 Final Data Collection and Analysis*

Final data collection for the PVT system involved measuring temperature and solar irradiance using a Solar System Data Logger and adjusting irradiance (400 W/m², 600 W/m², 800 W/m²) with a voltage regulator. Water mass flow rates (30 l/h, 60 l/h, 90 l/h) were set using a flow meter to find the optimal rate for the system. Temperature readings of the PVT module, and water channel inlets and outlets were recorded using PicoLog TC-08. The experiments were conducted separately to prevent accumulated heat and allow the PVT cell to cool down to ambient temperature before the next test for fair results. Efficiency calculations using equations for electrical, thermal, and overall efficiency were performed. The following equations will be used to determine the electrical, thermal, and overall efficiency.

$$P_{max} = V_{oc} \times I_{sc} \times FF \quad (1)$$

$$Fill\ Factor\ (FF) = \frac{V_{MPP} \times I_{MPP}}{V_{oc} \times I_{sc}} \quad (2)$$

$$V_{MPP} I_{MPP} = FF \times V_{oc} \times I_{sc} \quad (3)$$

$$\eta_{El} = \frac{P_{max}}{G \times A} = \frac{V_{MP} \times I_{MP}}{G \times A} = \frac{FF \times V_{OC} \times I_{SC}}{G \times A} \quad (4)$$

$$Q = \dot{m}_w C_{pw}(\Delta T) \tag{5}$$

where, $\Delta T = T_{out} - T_{in}$ (6)

$$\eta_{th} = \frac{Q}{G \times A} \tag{7}$$

$$\eta_{tot} = \frac{P}{G \times A} + \frac{Q}{G \times A} = \frac{(P+Q)}{G \times A} \tag{8}$$

### *2.5 Uncertainty Analysis*

An uncertainty analysis was conducted to ensure the accuracy and reliability of the experimental results. The uncertainties in the measurements of temperature, flow rate, solar irradiance, and electrical parameters were calculated and factored the efficiency calculations. The total uncertainty in the calculated efficiencies was determined using the Eq. (9).

$$W_R = \left[\left(\frac{\partial R}{\partial x_1} W_1\right)^2 + \left(\frac{\partial R}{\partial x_2} W_2\right)^2 + \cdots + \left(\frac{\partial R}{\partial x_n} W_n\right)^2\right]^{1/2} \tag{9}$$

where $W_r$ is the uncertainty for the function R of the independent linear variables ($x_1$, $x_2$, …, $x_n$), while the ($W_1$, $W_2$, …, $W_n$) denoted as uncertainties in these independent variables. The uncertainties of the measuring instruments used in the experimental setup are detailed in Table 6. In this research, the maximum uncertainties in the experiments are below 5%. As Hamada *et al.,* [19] mentioned that for low-risk engineering applications, the value of uncertainty is 5%. This demonstrated that the measuring instruments provides values within satisfactory and reliable engineering limits.

**Table 6**
Uncertainty of measuring instruments

| Measuring instrument | Measuring parameter | Uncertainty in experiment |
|---|---|---|
| Type-K Thermocouple | Temp. (Inlet & outlet) | ±0.1% |
| TC-08 Thermocouple Data Logger | Temperature (data logging) | ±0.5% |
| Flow Meter | Water Flow Rate | ±1% |
| Pyranometer | Solar Irradiance | ±1.5% |
| Array 3721A DC Electronic Load | Voltage | ±0.1% |
| | Current | ±0.1% |

## **3. Results**
### *3.1 Temperature Difference*

The results indicate that integrating commercial PCM and T-fin absorber into a PVT system significantly cooled down the operational temperature of the PVT module compared to a standard PV system. This cooling effect is shown by temperature drops across different irradiance levels and water flow rates. According to Table 7 and Figure 9, at 400 W/m$^2$, the PVT system with PCM exhibited average temperature drops of 3.28°C, 4.80°C, and 7.51°C for flow rates of 30 l/h, 60 l/h, and 90 l/h, respectively. At 600 W/m$^2$, these drops were 5.90°C, 6.78°C, and 7.85°C, and at 800 W/m$^2$, were 8.44°C, 10.64°C, and 11.20°C, respectively. The maximum temperature drop of 11.20°C or 14.36% at the highest irradiance level (800 W/m$^2$) and flow rate (90 l/h) compared to PV alone. These findings are consistent with studies by Abdul-Ganiyu *et al.,* [20] and Pang *et al.,* [21] showing that PCM integration and increasing water flow rates effectively reduced temperature differences, showing enhanced heat removal and cooling efficiency. Overall, the combination of PCM, T-Fin absorbers, and optimized flow rates successfully regulated temperatures and improved the thermal performance and efficiency of the system.

**Table 7**
Temperature drop of each irradiance level with varies mass flow rate

| Irradiance | Type of Cell | Water Flow Rate | Average Surface Temperature | Temperature Drop |
|---|---|---|---|---|
| 400 W/m$^2$ | PV | - | 59.49°C | (Reference) |
| | PVT + PCM | 30 l/h | 56.21°C | 3.28°C |
| | | 60 l/h | 54.69°C | 4.80°C |
| | | 90 l/h | 51.98°C | 7.51°C |
| 600 W/m$^2$ | PV | - | 73.50°C | (Reference) |
| | PVT + PCM | 30 l/h | 67.60°C | 5.90°C |
| | | 60 l/h | 66.72°C | 6.78°C |
| | | 90 l/h | 65.65°C | 7.85°C |
| 800 W/m$^2$ | PV | - | 78.02°C | (Reference) |
| | PVT + PCM | 30 l/h | 69.58°C | 8.44°C |
| | | 60 l/h | 67.38°C | 10.64°C |
| | | 90 l/h | 66.82°C | 11.20°C |

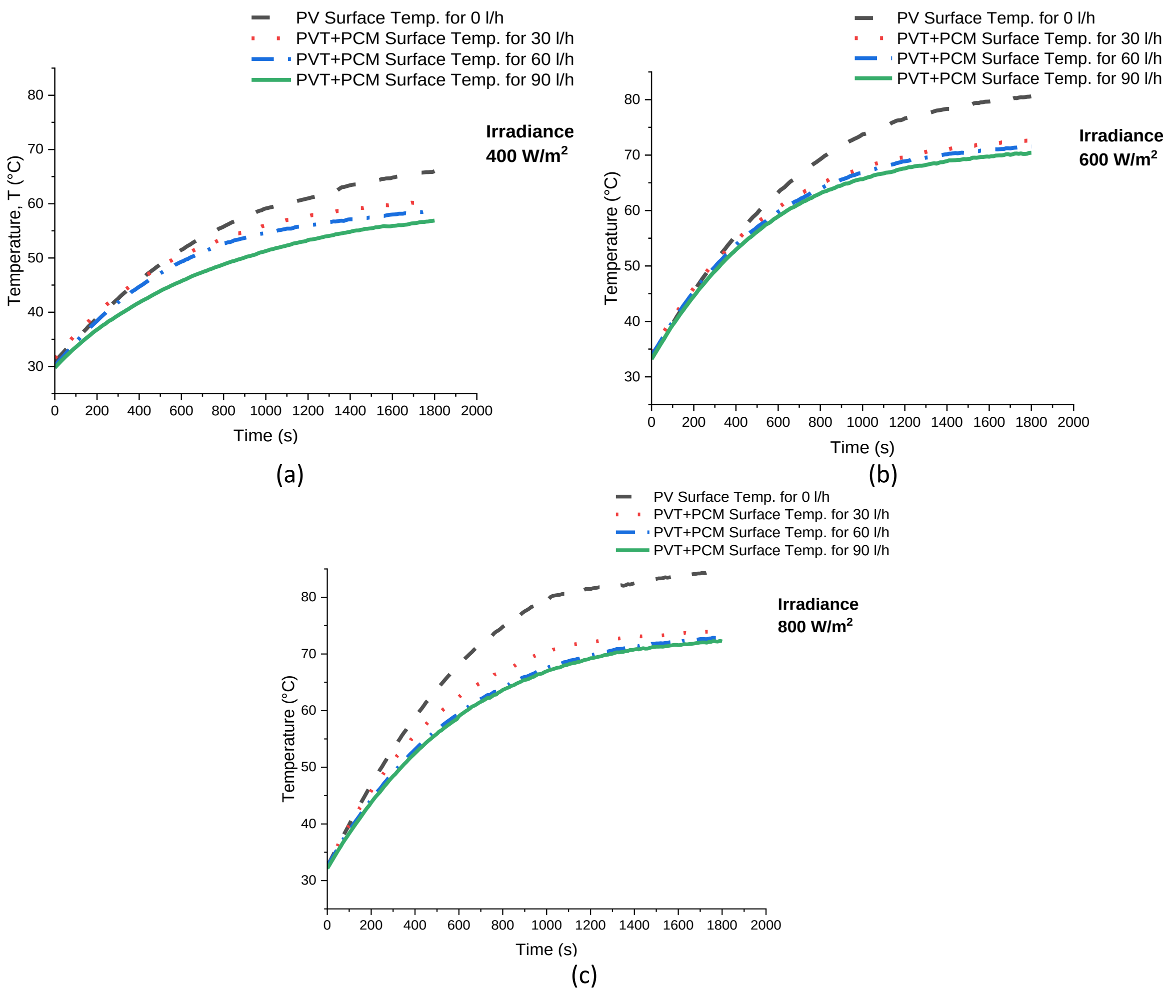


**Fig. 9.** Temperature difference with varies mass flow rates at (a) 400 W/m$^2$, (b) 600 W/m$^2$, (c) 800 W/m$^2$

### *3.2 Electrical Efficiency*

The analysis of electrical performance data at varying mass flow rates (0 l/h for PV and 30 l/h, 60 l/h, 90 l/h for PVT with PCM) and irradiance levels (400 W/m$^2$, 600 W/m$^2$, 800 W/m$^2$) shows significant increments in electrical efficiency when integrating phase change materials (PCM) with T-fin absorber. Based on Table 8, at an irradiance of 400 W/m$^2$, the average electrical efficiency increases from 5.585% for PV-only systems to 6.957%, 7.082%, and 7.245% for PVT with PCM systems at 30 l/h, 60 l/h, and 90 l/h flow rates, respectively. This trend continues at higher irradiances, with efficiencies at 600 W/m$^2$ rising from 6.017% (PV) to 7.016%, 7.170%, and 7.291%, and at 800 W/m$^2$ from 6.011% (PV) to 7.652%, 7.926%, and 8.020%.

**Table 8**
Electrical performance of systems with varies mass flow rates at each irradiance

| Type of Cell | Water Flow Rate | Electrical Parameter | Solar Irradiance | | |
|---|---|---|---|---|---|
| | | | 400W/m$^2$ | 600W/m$^2$ | 800W/m$^2$ |
| PV | - | Current ($I_{sc}$) | 0.416A | 0.651A | 0.869A |
| | | Voltage ($V_{oc}$) | 20.314V | 20.637V | 20.537V |
| | | Fill Factor (FF) | 0.743491 | 0.756042 | 0.758450 |
| | | Power (P) | 6.287W | 10.160W | 13.532W |
| | | Electrical Efficiency ($\eta_{EL}$) | 5.585% | 6.017% | 6.011% |
| PVT + PCM | 30 l/h | Current ($I_{sc}$) | 0.537A | 0.851A | 1.117A |
| | | Voltage ($V_{oc}$) | 20.037V | 19.642V | 20.033V |
| | | Fill Factor (FF) | 0.728575 | 0.709007 | 0.770842 |
| | | Power (P) | 7.830W | 11.845W | 17.226W |
| | | Electrical Efficiency ($\eta_{EL}$) | 6.957% | 7.016% | 7.652% |
| | 60 l/h | Current ($I_{sc}$) | 0.553A | 0.862A | 1.089A |
| | | Voltage ($V_{oc}$) | 19.864V | 19.575V | 21.144V |
| | | Fill Factor (FF) | 0.725151 | 0.717754 | 0.775284 |
| | | Power (P) | 7.971W | 12.106W | 17.842W |
| | | Electrical Efficiency ($\eta_{EL}$) | 7.082% | 7.170% | 7.926% |
| | 90 l/h | Current ($I_{sc}$) | 0.571A | 0.880A | 1.094A |
| | | Voltage ($V_{oc}$) | 19.735V | 19.541V | 21.177V |
| | | Fill Factor (FF) | 0.723264 | 0.716304 | 0.779366 |
| | | Power (P) | 8.155W | 12.310W | 18.054W |
| | | Electrical Efficiency ($\eta_{EL}$) | 7.245% | 7.291% | 8.020% |

According to the results in Table 8, these improvements can be attributed to the ability of PCM and the higher heat transfer rate of T-fin absorber to regulate temperature effectively and enhance electrical output. Additionally, the increased electrical efficiency, $\eta_{EL}$ at higher irradiance and mass flow rates are due to improved heat dissipation facilitated by the PCM and higher water flow rates [22]. Higher irradiance levels provide more energy for the photovoltaic cells to convert which can lead to higher electrical output. Simultaneously, increased mass flow rates improve the cooling efficiency, maintaining the cells at lower working temperatures and optimizing the performance of PVT system. These findings also aligned with the research by Zohora and Nasrin [23] and Nasrin *et al.,* [24]. The superior performance of the T-fin absorber design in maximizing heat transfer rate further supports the observed efficiency gains.

Based on Figure 10(a), the power output data at different irradiance levels (400 W/m$^2$, 600 W/m$^2$, 800 W/m$^2$) and water flow rates (0 l/h for PV and 30 l/h, 60 l/h, 90 l/h for PVT with PCM) shows considerable improvements on PVT with PCM configurations compared to PV-only setups. The power output consistently rises with higher irradiance levels and optimized water flow rates, from 6.287W (0 l/h at 400W/m$^2$) to 18.054W (90 l/h at 800 W/m$^2$) showing the significant potential for enhancing electrical efficiency. Elbreki *et al.,* [25] stated the maximum output power of a PV panel increases as solar radiation increases and Li *et al.,* [26] noted the temperature of the PV panel gradually decreases and the output power increases when the water flow rate exceeds 0.15 kg/s.

Figure 10(b) and Figure 10(c) show the results of electrical efficiency across different irradiance levels and water flow rates. At 90 l/h flow rate, the electrical efficiency increased from 7.245% (400 W/m$^2$) to 8.020% (800 W/m$^2$). This result is further supported by Abdullah *et al.,* [27] that mentioned an increase at irradiance level of 100 to 1000 W/m$^2$ caused efficiency increases by 11 to 11.6%. At 800 W/m$^2$, electrical efficiency increased from 6.011% (0 l/h of PV) to 8.020% (90 l/h of PVT with PCM). This finding pattern is proved by Tripty and Nasrin [28] that the electrical efficiency increased from 12.91% at 0.015 kg/s flow rate to 14.19% at 0.5 kg/s flow rate. The results show a consistent increase in electrical efficiency with higher water flow rates and irradiance levels. This illustrates the advantage of the high flow rate of the working fluid in optimizing thermal conditions for improved electrical performance.

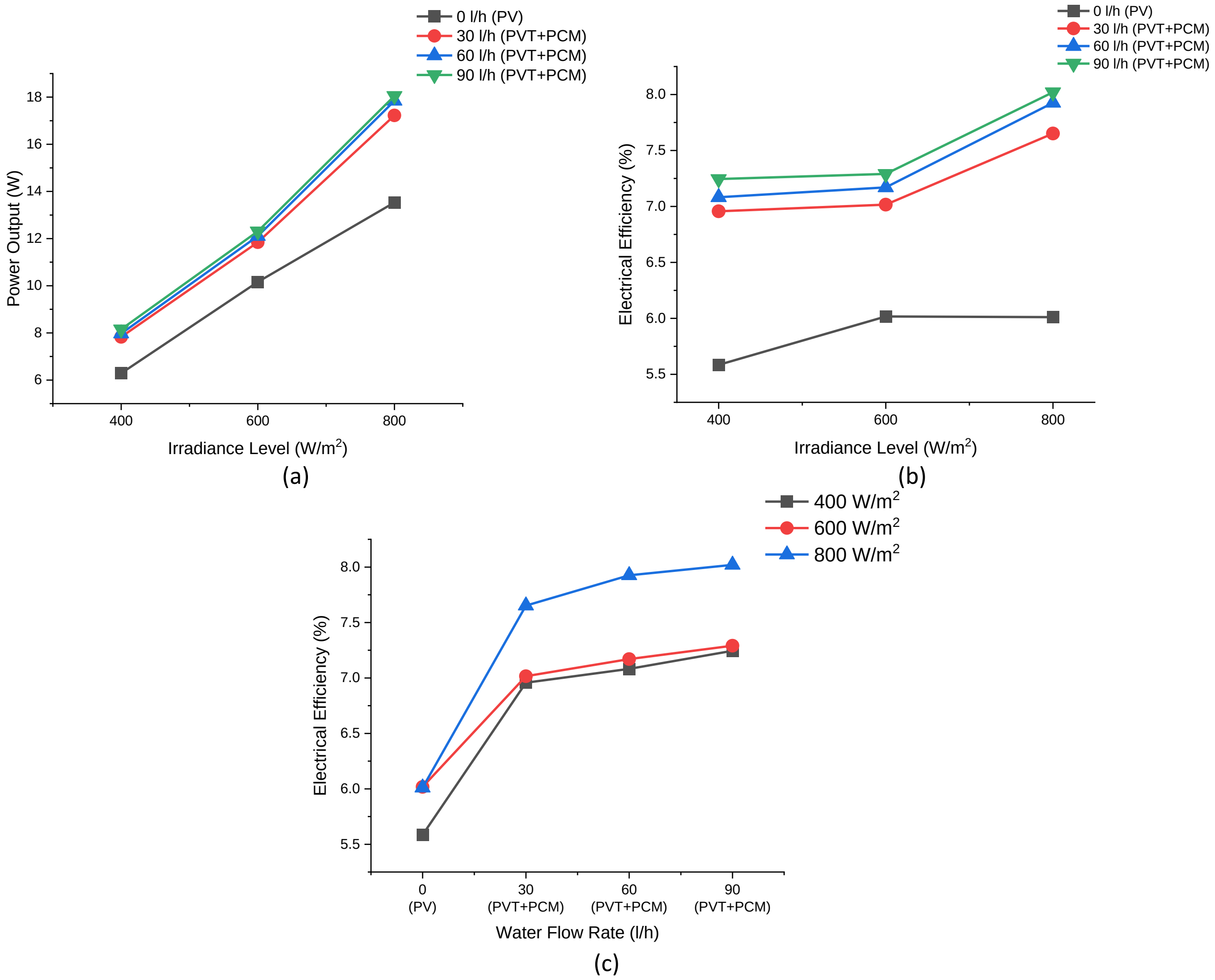


**Fig. 10.** (a) Power output vs. Irradiance level, (b) Electrical efficiency vs. Irradiance level, (c) Electrical efficiency vs. Water flow rate

### *3.3 Thermal Efficiency*

The thermal performance data for PVT with PCM systems across different irradiance levels (400 W/m$^2$, 600 W/m$^2$, 800 W/m$^2$) and water flow rates (30 l/h, 60 l/h, 90 l/h) showing a massive increase in thermal efficiency with higher mass flow rates, particularly at lower irradiance. According to Table 9, at 400 W/m$^2$, the thermal efficiency peaks at 72.519% for a 90 l/h flow rate, whereas at 600 W/m$^2$ and 800 W/m$^2$, the highest efficiencies are recorded at 62.395% and 54.544% respectively for the same flow rate.

**Table 9**
Thermal performance of systems with varies mass flow rates at each irradiance

| Type of Cell | Water Flow Rate | Thermal Parameter | Solar Irradiance | | |
|---|---|---|---|---|---|
| | | | 400W/m$^2$ | 600W/m$^2$ | 800W/m$^2$ |
| PVT + PCM | 30 l/h | Water Inlet Temperature ($T_{in}$) | 31.38°C | 36.07°C | 31.76°C |
| | | Water Outlet Temperature ($T_{out}$) | 32.08°C | 36.88°C | 32.79°C |
| | | Temperature Difference (ΔT) | 0.70°C | 0.81°C | 1.03°C |
| | | Heat Energy ($\dot{Q}$) | 24.417W | 28.254W | 35.928W |
| | | Thermal Efficiency ($\eta_{TH}$) | 21.693% | 16.734% | 15.960% |
| | 60 l/h | Water Inlet Temperature ($T_{in}$) | 32.75°C | 35.27°C | 28.30°C |
| | | Water Outlet Temperature ($T_{out}$) | 33.47°C | 36.10°C | 29.38°C |
| | | Temperature Difference (ΔT) | 0.72°C | 0.84°C | 1.08°C |
| | | Heat Energy ($\dot{Q}$) | 50.099W | 58.488W | 75.499W |
| | | Thermal Efficiency ($\eta_{TH}$) | 44.509% | 34.641% | 33.537% |
| | 90 l/h | Water Inlet Temperature ($T_{in}$) | 27.95°C | 35.88°C | 29.74°C |
| | | Water Outlet Temperature ($T_{out}$) | 28.73°C | 36.88°C | 30.91°C |
| | | Temperature Difference (ΔT) | 0.78°C | 1.01°C | 1.17°C |
| | | Heat Energy ($\dot{Q}$) | 81.627W | 105.348W | 122.790W |
| | | Thermal Efficiency ($\eta_{TH}$) | 72.519% | 62.395% | 54.544% |

Based on Table 9, the elevated thermal efficiency is caused by the increased heat extraction capacity at higher mass flow rates, which enhances the overall heat transfer and reduces thermal losses. This finding is further supported by research of Rahou *et al.,* [29] as stated that higher water mass flow rate increases the heat transfer between the water flow and the back plate. The highest thermal efficiency at the lowest irradiance is due to the reduced heat input, which allowing the cooling system to maintain a lower overall temperature and thus operate more efficiently. From Table 9 results, the thermal power increases when the irradiance increases but lead to a lower thermal efficiency due to significant increased heat input but with slightly increased heat output. This phenomenon also aligned with the study of Luan *et al.,* [30] as stated that higher solar irradiance increases thermal power but reduces thermal efficiency.

Additionally, the temperature difference between the water inlet and outlet (ΔT) also increases with higher irradiance and mass flow rates. This is because higher irradiance levels provide more thermal energy to be absorbed by the working fluid and resulting in a greater temperature rise of the water when passes through the system. Secondly, higher mass flow rates facilitate better heat transfer which allowing more thermal energy to be absorbed by the water in a given time period and further increasing ΔT. As the water flow rate increases, the capacity of the system to extract and dissipate heat improves. This causing a higher outlet temperature compared to the inlet temperature.

Based on Figure 11(a), the thermal efficiency results for PVT with PCM systems under varying irradiance levels and different water flow rates shows a clear trend where thermal efficiency increases significantly with higher flow rates but at lower irradiance. At 400 W/m$^2$, the thermal efficiency reaches 72.519% at a flow rate of 90 l/h. This trend is less pronounced at higher irradiance levels with thermal efficiency dropping to 62.395% and 54.544% for 600 W/m$^2$ and 800 W/m$^2$ respectively at the same flow rate, the trend also similar to other water flow rates. These results indicate the potential of lower irradiance condition for thermal efficiency gains is greater. These results also aligned with study of Zohri *et al.,* [31] where the highest thermal efficiency recorded was 64.30% at 500 W/m$^2$, while the lowest thermal efficiency observed was 56.34% at 1000 W/m$^2$. Hence, a decrease in solar irradiance will increase the thermal efficiency. Conversely, an increase in solar radiation will reduce the thermal efficiency.

As irradiance increases, the thermal efficiency decreases primarily due to a higher rate of heat loss to the surroundings. At higher irradiance levels, more heat is absorbed by the system, raising the temperature of both the photovoltaic (PV) panel and the phase change material (PCM). This results in higher thermal losses, especially through radiation and convection, as heat dissipates more easily from a system operating at elevated temperatures. Additionally, the heat stored in the PCM may reach its melting point faster, limiting the ability of PCM to absorb further heat and leading to faster dissipation. To minimize these losses, incorporating more effective insulation around the system could reduce heat dissipation. Another solution would be to optimize the cooling system by increasing water flow rates or integrating advanced cooling techniques like forced air cooling or nanofluid-based cooling. This would help maintain lower operational temperatures and improve the thermal management of system under high irradiance conditions.

Based on Figure 11(b), at all irradiance levels, increasing the water flow rate significantly enhances thermal efficiency. For instance, at an irradiance of 400 W/m$^2$, the thermal efficiency increases from 21.693% at 30 l/h to 72.519% at 90 l/h. A similar pattern is also observed at higher irradiance levels. At 600 W/m$^2$, efficiency rises from 16.734% to 62.395%, and at 800 W/m$^2$, from 15.960% to 54.544% when water flow rate increased. These results show the importance of optimizing water flow rates to achieve higher thermal efficiency. These results also aligned with research by Fudholi *et al.,* [32] where the thermal efficiency increase from 58.01% to 68.42% when the mass flow rate increased from 0.011 kg/s to 0.041 kg/s.

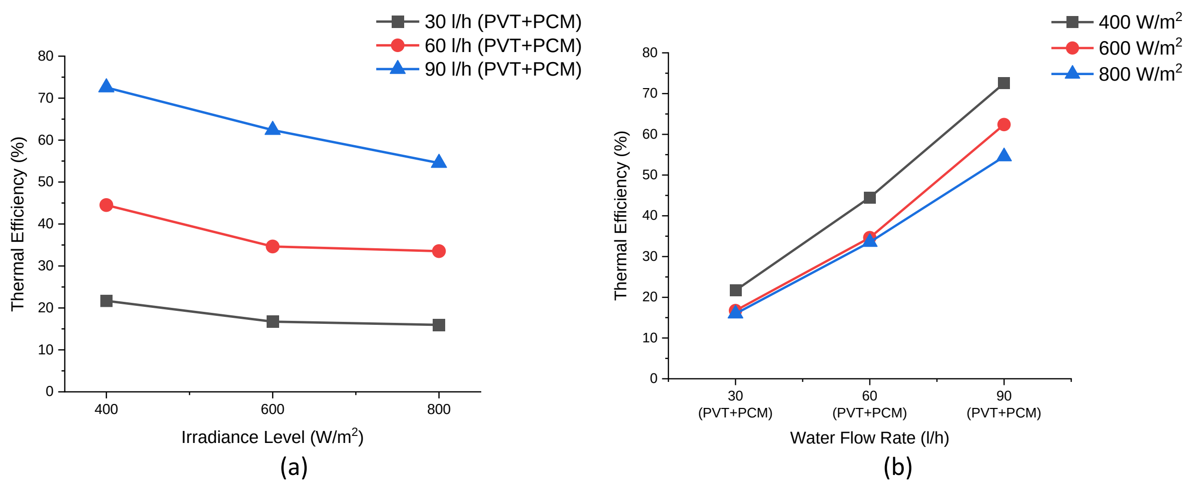


**Fig. 11.** (a) Thermal efficiency vs. Irradiance level, (b) Thermal efficiency vs. Water flow rate

### *3.4 Overall Efficiency*

The overall performance of photovoltaic thermal (PVT) systems integrated with phase change materials (PCM) at varying irradiance levels (400 W/m$^2$, 600 W/m$^2$, 800 W/m$^2$) and water flow rates (30 l/h, 60 l/h, 90 l/h) shows significant enhancements in both electrical and thermal efficiencies compared to standalone photovoltaic (PV) cells. According to Table 10, at an irradiance of 400 W/m$^2$ and a water flow rate of 90 l/h, the PVT with PCM system achieves the highest overall efficiency of 79.764% due to the highest thermal efficiency of 72.519% and an electrical efficiency of 7.245%. At 800 W/m$^2$ and 90 l/h, the system achieved the highest electrical efficiency of 8.020%, but with lower thermal efficiency of 54.544%, therefore contributing to a lower overall efficiency of 62.564%.

**Table 10**
Overall performance of systems with varies mass flow rates at each irradiance

| Type of Cell | Water Flow Rate | Parameter | Solar Irradiance | | |
|---|---|---|---|---|---|
| | | | 400W/m$^2$ | 600W/m$^2$ | 800W/m$^2$ |
| PV | - | Electrical Efficiency ($\eta_{EL}$) | 5.585% | 6.017% | 6.011% |
| | | Thermal Efficiency ($\eta_{TH}$) | - | - | - |
| | | Overall Efficiency ($\eta_{Total}$) | 5.585% | 6.017% | 6.011% |
| PVT + PCM | 30 l/h | Electrical Efficiency ($\eta_{EL}$) | 6.957% | 7.016% | 7.652% |
| | | Thermal Efficiency ($\eta_{TH}$) | 21.693% | 16.734% | 15.960% |
| | | Overall Efficiency ($\eta_{Total}$) | 28.650% | 23.750% | 23.612% |
| | 60 l/h | Electrical Efficiency ($\eta_{EL}$) | 7.082% | 7.170% | 7.926% |
| | | Thermal Efficiency ($\eta_{TH}$) | 44.509% | 34.641% | 33.537% |
| | | Overall Efficiency ($\eta_{Total}$) | 51.591% | 41.811% | 41.463% |
| | 90 l/h | Electrical Efficiency ($\eta_{EL}$) | 7.245% | 7.291% | 8.020% |
| | | Thermal Efficiency ($\eta_{TH}$) | 72.519% | 62.395% | 54.544% |
| | | Overall Efficiency ($\eta_{Total}$) | 79.764% | 69.686% | 62.564% |

The integration of PCM in PVT systems helps in stabilizing the temperature, thus maintaining higher efficiency under varying irradiance levels. The data in Table 10 shows the importance of optimizing both the flow rate and the use of PCM to maximize the overall efficiency of PVT systems at a specific range of irradiance. The data obtained in this research is further supported by statement of Alsalame *et al.,* [33] that stated the PVT system had a higher overall efficiency than the PV system and the improvement of the thermal energy alone can sufficiently increase the overall performance of the system.

Based on Figure 12(a), the overall efficiency of PVT system integrated with PCM decreased with increasing of irradiance levels as observed in the obtained data. At 30 l/h flow rate, the overall efficiency of the system decreases from 28.650% to 23.612% for the PVT with PCM system when irradiance level is increasing from 400 W/m$^2$ to 800 W/m$^2$. This trend is similar across different water flow rates such as 60 l/h and 90 l/h, at 60 l/h, the overall efficiency drops from 51.591% to 41.463%, and at 90 l/h, from 79.764% to 62.564% when the irradiance is increasing from 400 W/m$^2$ to 800 W/m$^2$. These results were aligned with the research of Prabowo *et al.,* [31] that the recorded maximum overall PVT efficiency is 76.23% at 500 W/m$^2$ low irradiance. Conversely, the lowest overall PVT efficiency of 69.34% is at a 1000 W/m$^2$ high irradiance. This decline can be explained by the increased thermal stress on the PV cells at higher irradiance levels, which increases the heat power input and negatively impacts thermal efficiency. Additionally, while the PCM helps to some extent, the heat removal capacity of the system is not be sufficient to counteract the higher thermal loads at high irradiance levels which causing overall efficiency to reduce.

Based on Figure 12(b), the overall efficiency of PVT system integrated with PCM significantly improved with increasing of water flow rates as observed in the obtained data. At 400 W/m$^2$

irradiance, the overall efficiency of the system increases from 5.585% for a standalone PV cell to 79.764% for the PVT with PCM system when 90 l/h water flow rate. This trend is consistent across different irradiance levels, at 600 W/m$^2$, the efficiency rises from 6.017% to 69.686% as the flow rate rises from 0 l/h to 90 l/h, and at 800 W/m$^2$, from 6.011% without any cooling water and method to 62.564% with maximum cooling water flow rate, PCM and T-fin absorber. These findings also aligned with the research of Rukman *et al.,* [34] where stated both electrical and thermal efficiencies increased when the mass flow rate increased, hence the overall efficiency increased simultaneously when the mass flow rate increased. Rukman *et al.,* [34] obtained overall PVT efficiency of 75% to 90% when the flow rate is ranging from 0.012 kg/s to 0.0255 kg/s. This substantial improvement indicates that higher flow rates enhance the cooling of the PV cells, thereby reducing the operating temperature and improving both electrical and thermal efficiencies. This data shows the importance of optimizing water flow rates to balance the thermal load and maintain higher efficiency under varying irradiance conditions.

Overall, the best overall efficiency of 79.8% is achieved at lowest irradiance 400W/m$^2$ and highest mass flow rate 90 l/h. This result is similar with the study by Zohri *et al.,* [31], where the highest overall efficiency of 76.23% is observed when the irradiance is lowest at 500 W/m$^2$ and water mass flow rate is highest at 0.009 kg/s. On the other hand, the lowest overall efficiency is observed at highest irradiance 1000 W/m$^2$ and lowest water mass flow rate 0.001 kg/s. The fundamental of optimum overall efficiency at lowest irradiance is because of high irradiance caused the thermal load and heat input increases significantly, but the cooling water difficult to absorb the excess heat effectively. On the other side, the fundamental of optimum overall efficiency at highest mass flow rate is because of low water flow rate has insufficient cooling efficiency leads to higher operating temperatures and resulting in lower electrical and thermal efficiencies and thus lower overall efficiency.

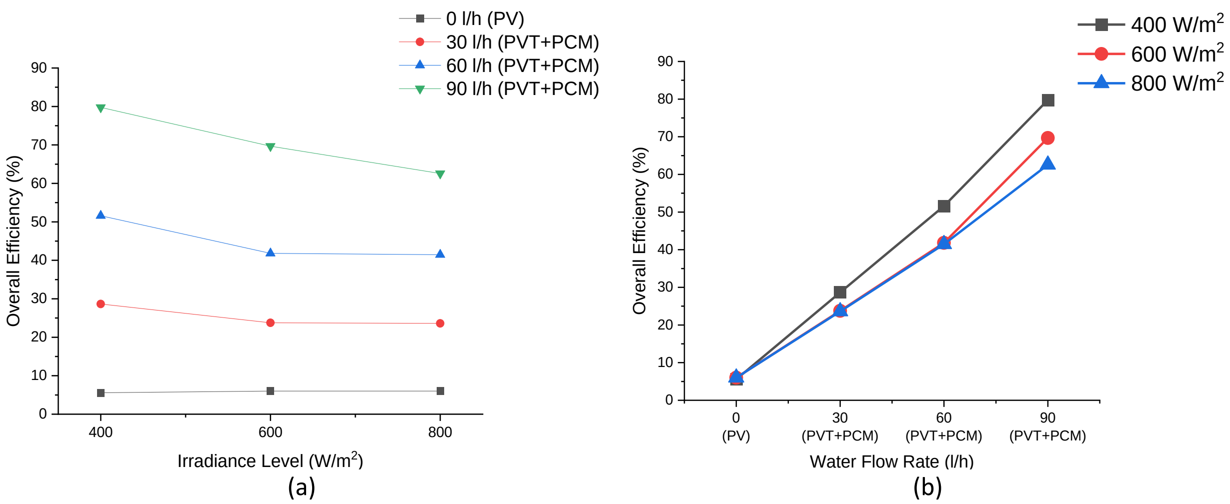


**Fig. 12.** (a) Overall efficiency vs. Irradiance level, (b) Overall efficiency vs. Water flow rate

## 4. Conclusions

In conclusion, this research successfully developed and evaluated the efficiency of a PVT system integrated with commercial PCM using a copper T-fin absorber to enhance solar energy conversion. The study involved fabricating aluminum packets for commercial PCM, incorporating these packets into the PVT container, and conducting experiments under three different water flow rates which are 30 l/h, 60 l/h, and 90 l/h at three different irradiance levels which are 400 W/m$^2$, 600 W/m$^2$, and 800 W/m$^2$ using indoor solar simulator. The results presented substantial improvements in both electrical and thermal efficiencies. The highest temperature drop of 11.20°C was achieved at 800 W/m² and 90 l/h due to enhanced cooling system. The system achieved the highest electrical efficiency of 8.0% at 800 W/m² and 90 l/h, and the highest thermal efficiency of 72.5% at 400 W/m² and 90 l/h. The overall efficiency peaked at 79.8% under 400 W/m² and 90 l/h proving the ability to effectively convert solar energy of the system. Nevertheless, the overall efficiency still achieved high value of 62.6% when the flow rate is 90 l/h compared to 30 l/h and 60 l/h at high irradiance of 800 W/m². At mass flow rate of 90 l/h and an irradiance level of 400 W/m$^2$ can be recognized as the optimum parameter values for best performance of the PVT system using T-fin absorber design.

Scaling the current PVT system for commercial applications could present several challenges, primarily due to differences between controlled experimental conditions and real-world environments. In a controlled setting, parameters such as irradiance, water flow rate, and cooling are optimized. However, in real-world applications, fluctuating solar irradiance, varying ambient temperatures, and inconsistent water supply could lead to less predictable performance. Additionally, the integration of copper T-fin absorbers and commercial PCM could increase manufacturing costs and complexity, especially for large-scale production. To address these issues, further research on optimizing material costs, enhancing system durability, and improving heat transfer at larger scales would be necessary. Potential solutions may involve using more cost-effective materials, refining the cooling system design, or integrating automated control systems to adapt to varying environmental conditions.

The integration of PCM and the copper T-fin absorber in the PVT system was chosen to enhance thermal regulation and improve overall efficiency. However, this integration inevitably increases the complexity and cost of the system. The copper T-fin absorber offers high thermal conductivity, enhancing heat dissipation and boosting thermal efficiency, while the PCM helps stabilize temperature fluctuations, especially at higher irradiance levels. The cost of copper and the commercial PCM is a key consideration, as copper is more expensive than alternative materials. However, the increased efficiency gain, particularly in electrical and overall energy conversion, offsets some of these costs, making the system more efficient and reliable under variable environmental conditions. Future work could explore cost reductions through material substitution, such as using aluminum fins or optimizing the design for easier manufacturing. A more detailed economic analysis including return on investment is needed to determine the full cost-benefit ratio for large-scale applications.

The lifetime environmental impact of the PVT system also been considered, particularly regarding the materials used, such as the copper T-fin absorber and the commercial PCM. Copper is known for durability and recyclability, which is a sustainable choice for long-term use despite the initial extraction impact. The commercial PCM used in the system is non-toxic and has a long lifespan, reducing the need for frequent replacement and minimizing waste. However, the manufacturing process of copper and PCM does have a carbon footprint. Future optimization could explore using alternative, less resource-intensive materials, such as recycled metals or bio-based PCMs to further reduce environmental impact. Additionally, the high efficiency in solar energy conversion could offset the environmental impact over time by generating clean energy and reducing reliance on fossil fuels.

**Acknowledgement**
The author would like to express heartfelt gratitude to Universiti Teknikal Malaysia Melaka (UTeM), the Faculty of Mechanical Technology and Engineering (FTKM), and the Applied Solar Energy Laboratory (ASEL) for their invaluable support in making this research possible.

## References

[1] Rahman, M. M., Md Hasanuzzaman, and Nasrudin Abd Rahim. "Effects of various parameters on PV-module power and efficiency." *Energy Conversion and Management* 103 (2015): 348-358. https://doi.org/10.1016/j.enconman.2015.06.067

[2] Saurabh, Ashish, Deepali Atheaya, and Anil Kumar. "Study of hybrid photovoltaic thermal systems." In *IOP Conference Series: Materials Science and Engineering*, vol. 748, no. 1, p. 012016. IOP Publishing, 2020. https://doi.org/10.1088/1757-899X/748/1/012016

[3] Jia, Yuting, Guruprasad Alva, and Guiyin Fang. "Development and applications of photovoltaic-thermal systems: A review." *Renewable and Sustainable Energy Reviews* 102 (2019): 249-265. https://doi.org/10.1016/j.rser.2018.12.030

[4] Rubbi, Fazlay, Likhan Das, Khairul Habib, Navid Aslfattahi, R. Saidur, and Md Tauhidur Rahman. "State-of-the-art review on water-based nanofluids for low temperature solar thermal collector application." *Solar Energy Materials and Solar Cells* 230 (2021): 111220. https://doi.org/10.1016/j.solmat.2021.111220

[5] Abouel Nasr, Emad, Haitham A. Mahmoud, Mohammed A. El-Meligy, Emad Mahrous Awwad, Sachin Salunkhe, Vishal Naranje, R. Swarnalatha, and Jaber E. Abu Qudeiri. "Electrical efficiency investigation on photovoltaic thermal collector with two different coolants." *Sustainability* 15, no. 7 (2023): 6136. https://doi.org/10.3390/su15076136

[6] Ahmadi, Rouhollah, Farhad Monadinia, and Mahdi Maleki. "Passive/active photovoltaic-thermal (PVT) system implementing infiltrated phase change material (PCM) in PS-CNT foam." *Solar Energy Materials and Solar Cells* 222 (2021): 110942. https://doi.org/10.1016/j.solmat.2020.110942

[7] Muthukumar, Palanisamy, and Hakeem Niyas. "Materials, Design and Development of Latent Heat Storage Systems for Medium and Large-Scale Applications: Issues and Challenges." *Encyclopedia of Renewable and Sustainable Materials* (2020): 417-437. https://doi.org/10.1016/B978-0-12-803581-8.11154-3

[8] Liang, Jiyuan, Xuelai Zhang, and Jun Ji. "Hygroscopic phase change composite material--a review." *Journal of Energy Storage* 36 (2021): 102395. https://doi.org/10.1016/j.est.2021.102395

[9] Ma, Tao, Hongxing Yang, Yinping Zhang, Lin Lu, and Xin Wang. "Using phase change materials in photovoltaic systems for thermal regulation and electrical efficiency improvement: A review and outlook." *Renewable and Sustainable Energy Reviews* 43 (2015): 1273-1284. https://doi.org/10.1016/j.rser.2014.12.003

[10] Alsaqoor, Sameh, Ahmad Alqatamin, Ali Alahmer, Zhang Nan, Yaseen Al-Husban, and Hussam Jouhara. "The impact of phase change material on photovoltaic thermal (PVT) systems: A numerical study." *International Journal of Thermofluids* 18 (2023): 100365. https://doi.org/10.1016/j.ijft.2023.100365

[11] Kazem, Hussein A., AliH A. Al-Waeli, Miqdam T. Chaichan, Kamaruzzaman Sopian, and Ahmed A. Al-Amiery. "Enhancement of photovoltaic module performance using passive cooling (Fins): A comprehensive review." *Case Studies in Thermal Engineering* 49 (2023): 103316. https://doi.org/10.1016/j.csite.2023.103316

[12] Shoaib, Muhammad, Sheher Yar Khan, Naveed Ahmed, Mariam Mahmood, Adeel Waqas, Mumtaz A. Qaisrani, and Nadia Shehzad. "Thermal management of solar photovoltaic module by using drilled cylindrical rods integrated with phase change materials." *Journal of Energy Storage* 52 (2022): 104956. https://doi.org/10.1016/j.est.2022.104956

[13] Bayrak, Fatih, Hakan F. Oztop, and Fatih Selimefendigil. "Effects of different fin parameters on temperature and efficiency for cooling of photovoltaic panels under natural convection." *Solar Energy* 188 (2019): 484-494. https://doi.org/10.1016/j.solener.2019.06.036

[14] Khodadadi, Mohammadjavad, and M. Sheikholeslami. "Assessment of photovoltaic thermal unit equipped with phase change material in different finned containers." *Journal of Energy Storage* 46 (2022): 103939. https://doi.org/10.1016/j.est.2021.103939

[15] Chavan, Sachin V., and D. Devaprakasam. "Improving the performance of solar photovoltaic thermal system using phase change material." *Materials Today: Proceedings* 46 (2021): 5036-5041. https://doi.org/10.1016/j.matpr.2020.10.406

[16] Alipour, Navid, Bahram Jafari, and Khashayar Hosseinzadeh. "Analysis of the impact of metal foam with phase change material on solar photovoltaic thermal system efficiency." *Journal of Energy Storage* 98 (2024): 113064. https://doi.org/10.1016/j.est.2024.113064

[17] Bassam, Abdulsahib M., Kamaruzzaman Sopian, Adnan Ibrahim, Mohd Faizal Fauzan, Anwer B. Al-Aasam, and Ghaith Yahay Abusaibaa. "Experimental analysis for the photovoltaic thermal collector (PVT) with nano PCM and micro-fins tube nanofluid." *Case Studies in Thermal Engineering* 41 (2023): 102579. https://doi.org/10.1016/j.csite.2022.102579

[18] Mahdi, Zainab M., Ali N. Al-Shamani, Ahmed Al-Manea, Hazim A. Al-zurfi, Raed Al-Rbaihat, K. Sopian, and Ali Alahmer. "Enhancing photovoltaic thermal (PVT) performance with hybrid solar collector using phase change

material, porous media, and nanofluid." *Solar Energy* 283 (2024): 112983. https://doi.org/10.1016/j.solener.2024.112983

[19] Hamada, Alaa, Mohamed Emam, H. A. Refaey, M. Moawed, and M. A. Abdelrahman. "Investigating the performance of a water-based PVT system using encapsulated PCM balls: An experimental study." *Energy* 284 (2023): 128574. https://doi.org/10.1016/j.energy.2023.128574

[20] Abdul-Ganiyu, Saeed, David A. Quansah, Emmanuel W. Ramde, Razak Seidu, and Muyiwa S. Adaramola. "Study effect of flow rate on flat-plate water-based photovoltaic-thermal (PVT) system performance by analytical technique." *Journal of Cleaner Production* 321 (2021): 128985. https://doi.org/10.1016/j.jclepro.2021.128985

[21] Pang, Wei, Yanan Cui, Qian Zhang, Hongwen Yu, Linrui Zhang, and Hui Yan. "Experimental effect of high mass flow rate and volume cooling on performance of a water-type PV/T collector." *Solar Energy* 188 (2019): 1360-1368. https://doi.org/10.1016/j.solener.2019.07.024

[22] Rosli, Mohd Afzanizam Mohd, Muhammad Zaid Nawam, Irfan Alias Farhan Latif, Safarudin Ghazali Herawan, Noriffah Md Noh, Siti Nur Dini Noordin Saleem, and Faridah Hussain. "The Effect of variation in mass flow rate and solar irradiance on temperature uniformity and thermal performance of photovoltaic thermal: A simulated CFD study." *Journal of Advanced Research in Fluid Mechanics and Thermal Sciences* 91, no. 2 (2022): 106-119. https://doi.org/10.37934/arfmts.91.2.106119

[23] Zohora, F. T., and R. Nasrin. "A numerical analogy of improving efficiency for the PVT system in Bangladesh." *International Journal of Photoenergy* 2022, no. 1 (2022): 1901925. https://doi.org/10.1155/2022/1901925

[24] Nasrin, Rehena, Md Hasanuzzaman, and Nasrudin Abd Rahim. "Effect of high irradiation and cooling on power, energy and performance of a PVT system." *Renewable Energy* 116 (2018): 552-569. https://doi.org/10.1016/j.renene.2017.10.004

[25] Elbreki, Alghoul M., M. A. Alghoul, A. N. Al-Shamani, A. A. Ammar, Bita Yegani, Alsanossi M. Aboghrara, M. H. Rusaln, and Kamaruzzaman Sopian. "The role of climatic-design-operational parameters on combined PV/T collector performance: A critical review." *Renewable and Sustainable Energy Reviews* 57 (2016): 602-647. https://doi.org/10.1016/j.rser.2015.11.077

[26] Li, Manfeng, Zongshuai Yang, Lanjing Lu, Kui Yin, and Yiji Lu. "Investigation on Thermal and Electrical Performance of Late-Model Plate-and-Tube in Water-Based PVT-PCM Collectors." *Sustainability* 15, no. 7 (2023): 5988. https://doi.org/10.3390/su15075988

[27] Abdullah, Amira Lateef, Suhaimi Misha, Noreffendy Tamaldin, Mohd Afzanizam Mohd Rosli, and Fadhil Abdulameer Sachit. "A Review: Parameters affecting the PVT collector performance on the thermal, electrical, and overall efficiency of PVT system." *Journal of Advanced Research in Fluid Mechanics and Thermal Sciences* 60, no. 2 (2019): 191-232.

[28] Tripty, T. A., and R. Nasrin. "Efficiency upgrading of solar PVT finned hybrid system in Bangladesh: Flow rate and temperature influences." *Heliyon* 10, no. 7 (2024). https://doi.org/10.1016/j.heliyon.2024.e28323

[29] Rahou, M., M. Y. Othman, S. Mat, and A. Ibrahim. "Performance study of a photovoltaic thermal system with an oscillatory flow design." *Journal of Solar Energy Engineering* 136, no. 1 (2014): 011012. https://doi.org/10.1115/1.4024743

[30] Luan, Zhaoyang, Lanlan Zhang, Xiangfei Kong, Han Li, and Man Fan. "Experimental evaluation of factors affecting performance of concentrating photovoltaic/thermal system integrated with phase-change materials (PV/T-CPCM)." *Energy Storage and Saving* 3, no. 1 (2024): 30-41. https://doi.org/10.1016/j.enss.2023.06.001

[31] Zohri, Muhammad, Prabowo Prabowo, Suwarno Suwarno, Ahmad Fudholi, Sena Abraham Irsyad, Ajeng Tri Rahayu, Yadi Radiansah, Dalmasius Ganjar Subagio, Yusuf Suryo Utomo, and Aep Saepudin. "Simulation Approach of Photovoltaic Thermal Based on Water Collector with Rectangular Model." *CFD Letters* 16, no. 8 (2024): 121-137. https://doi.org/10.37934/cfdl.16.8.121137

[32] Fudholi, Ahmad, Kamaruzzaman Sopian, Mohammad H. Yazdi, Mohd Hafidz Ruslan, Adnan Ibrahim, and Hussein A. Kazem. "Performance analysis of photovoltaic thermal (PVT) water collectors." *Energy Conversion and Management* 78 (2014): 641-651. https://doi.org/10.1016/j.enconman.2013.11.017

[33] Alsalame, Haedr Abdalha Mahmood, Joo Hee Lee, and Gwi Hyun Lee. "Performance Evaluation of a Photovoltaic Thermal (PVT) system using nanofluids." Energies 14, no. 2 (2021): 301. https://doi.org/10.3390/en14020301

[34] Rukman, Nurul Shahirah Binti, Ahmad Fudholi, Nur Farhana Mohd Razali, Mohd Hafidz Ruslan, and Kamaruzzaman opian. "Energy and exergy analyses of photovoltaic-thermal (PV/T) system with $TiO_2$/water nanofluid flow." In *IOP Conference Series: Earth and Environmental Science*, vol. 268, no. 1, p. 012075. IOP Publishing, 2019. https://doi.org/10.1088/1755-1315/268/1/012075